Published in final edited form as:
Free Radic Biol Med. 2009 August 15; 47(4): 458–467. doi:10.1016/j.freeradbiomed.2009.05.019.

Chemical Model Systems for Cellular Nitros(yl)ation Reactions

Andreas Daiber[a,*,#], **Stefan Schildknecht**[b,*], **Johanna Müller**[a], **Markus M. Bachschmid**[c], and **Volker Ullrich**[b]

[a]2nd Medical Clinic, Department of Cardiology, Johannes Gutenberg University, Mainz, Germany

[b]Department of Biology, University of Konstanz, Germany

[c]Department of Medicine, Whitaker Cardiovascular Institute, Boston University School of Medicine, MA, USA

Abstract

S-nitros(yl)ation belongs to the redox-based posttranslational modifications of proteins but the underlying chemistry is controversial. In contrast to current concepts involving the autoxidation of nitric oxide ($^{\bullet}NO$, nitrogen monoxide), we and others have proposed the formation of peroxynitrite (oxoperoxonitrate(1-)) as an essential intermediate. This requires low cellular fluxes of $^{\bullet}NO$ and superoxide ($^{\bullet}O_2^-$), for which model systems have been introduced. We here propose two new systems for nitros(yl)ation that avoid the shortcomings of previous models. Based on the thermal decomposition of 3-morpholinosydnonimine, equal fluxes of $^{\bullet}NO$ and $^{\bullet}O_2^-$ were generated and modulated by the addition of $^{\bullet}NO$ donors or Cu,Zn-superoxide dismutase. As reactants for *S*-nitros(yl)ation, $NADP^+$-dependent isocitrate dehydrogenase and glutathione were employed, for which optimal *S*-nitros(yl)ation was observed at nanomolar fluxes of $^{\bullet}NO$ and $^{\bullet}O_2^-$ at a ratio of about 3:1. The previously used reactants phenol and diaminonaphthalene, (*C*- and *N*-nitrosation) demonstrated potential participation of multiple pathways for nitros(yl)ation. According to our data, neither peroxynitrite nor autoxidation of $^{\bullet}NO$ was as efficient as the $3^{\bullet}NO/1^{\bullet}O_2^-$ system in mediating *S*-nitros(yl)ation. In theory this could lead to an elusive nitrosonium (nitrosyl cation)-like species in the first step and to N_2O_3 in the subsequent reaction. Which of these two species or whether both together will participate in biological *S*-nitros(yl)ation remains to be elucidated. Finally, we developed several hypothetical scenarios to which the described U flux model could apply, providing conditions that allow either direct electrophilic substitution at a thiolate or *S*-nitros(yl)ation via transnitrosation from S-nitrosoglutathione.

Keywords

Nitric oxide; Superoxide; Peroxynitrite; Nitrosation reactions; *S*-nitrosylation; Nitrosophenol; Diaminonaphthalene; Free radicals

[#]Address correspondence to: Dr. Andreas Daiber, Klinikum der Johannes Gutenberg-Universität Mainz, II., Medizinische Klinik – Labor für Molekulare Kardiologie, Verfügungsgebäude für, Forschung und Entwicklung – Raum 00349, Obere Zahlbacher Str. 63, 55101 Mainz, Germany, Phone +49 (0)6131 33301, Fax +49 (0)6131 33304, andreas.daiber@bioredox.com.
[*]Both authors contributed equally and should be considered as first author.

With the nomenclature "*S*-nitros(yl)ation" that we use throughout the article, we conform with the numerous publications on biological *S*-nitros(yl)ation. However, this term does not reflect the important difference between "nitrosylation" caused by addition of $^{\bullet}NO$ to metal centers and "nitrosation" at a nucleophilic carbon, nitrogen, or sulfur atom leading to formal esters of nitrous acid.

Introduction

Redox regulation comprises several chemical mechanisms of oxidative or reductive modifications of proteins involved in the regulation of metabolic or biosynthetic pathways. These modifications include zinc-finger oxidation, methionine sulfoxidation, and oxidation or nitration of tyrosine residues [1], which all can be assigned to peroxynitrite derived from equal fluxes of nitric oxide (nitrogen monoxide, $^{\bullet}NO$) and superoxide anion ($^{\bullet}O_2^-$). The high reactivity of peroxynitrite ($ONOO^-$) allows such posttranslational modifications to occur in the submicromolar range and hence under physiological conditions [2,3].

An abundant posttranslational modification is *S*-nitros(yl)ation of Cys residues in proteins and low-molecular-weight thiols such as glutathione. Although *S*-nitros(yl)ation is abundant under physiological and pathophysiological conditions [4–7], neither are the underlying mechanisms well understood nor is there a unifying hypothesis on its physiological significance [8]. Because many enzymes rely on thiols as essential catalytic or structural groups, an inhibition but also an activation could be a consequence, as exemplified by the regulation of the NMDA receptor [9], HIF [10], or NF-κB [11], which have all been reported to involve *S*-nitros(yl)ation. According to the pioneering work of Stamler *et al.* [12,13], it can be assumed that enhanced biosynthesis of $^{\bullet}NO$ during cellular activation leads to a distinct nitros(yl)ation pattern in which glutathione (GSH) may be a primary target of a still elusive nitrosating agent [14]. By a mechanism of transnitros(yl)ation, other proteins containing consensus sequences for *S*-nitrosoglutathione (GSNO) binding may follow [15]. This hypothesis is supported by the high pK_a value of GSH and hence a high group transfer potential of GSNO to thiols or thiolates of proteins with low pK_a values. *N*-nitrosation has also been observed under cellular conditions, thus allowing the conclusion that an elusive nitrosating species exhibits a broad target spectrum [16–19]. However, there are no literature data available on the physiological relevance of N-nitroso species.

Formally, nitros(yl)ation proceeds by the reaction of a nitrosonium ion (NO^+) with a nucleophilic group (Eq. 1), but it is generally understood that in a physiological pH range, NO^+ is not stable but immediately forms nitrite (dioxonitrate(1-)) (Eq. 1a):

$$R{-}XH{+}[NO^+] \rightarrow R{-}X{-}NO{+}H^+ \quad (1)$$

$$[NO^+]{+}OH^- \rightarrow {NO_2}^- \quad (1a)$$

However, dinitrogen trioxide (N_2O_3), the anhydride of nitrous acid, is a well-known nitrosating agent that can be formed from $^{\bullet}NO$ and the $^{\bullet}NO_2$ radical (Eq. 3). The latter may arise as an autoxidation product of $^{\bullet}NO$ in the presence of dioxygen (Eq. 2) but this reaction is second order with regard to $^{\bullet}NO$ and hence becomes very slow at physiological concentrations of $^{\bullet}NO$ [20]. Therefore the autoxidation of $^{\bullet}NO$ with subsequent formation of N_2O_3 seems to be an implausible model for biological *S*-nitros(yl)ation:

$$2\,{}^{\bullet}NO{+}O_2 \rightarrow 2\,{}^{\bullet}NO_2 \quad (2)$$

$$^{\bullet}NO_2 + {}^{\bullet}NO \rightarrow N_2O_3 \quad (3)$$

This also renders the alternative mechanism of electron abstraction from a thiolate by $^{\bullet}NO_2$ or $^{\bullet}O_2^-$ unlikely [21]. Recent reports showing thiyl radical trapping in the presence of peroxynitrite [22] used high concentrations of peroxynitrite in the presence of CO_2, which easily leads to homolytic cleavage [23] of the CO_2/peroxynitrite adduct. It has been pointed out repeatedly that bolus additions of peroxynitrite may give erroneous results compared to the generation of peroxynitrite by low fluxes of $^{\bullet}NO$ and $^{\bullet}O_2^-$ as seen under physiological conditions [24]. However, recent kinetic data were in favor of thiyl-mediated *S*-nitros(yl)ation, requesting consideration of this pathway as well [25].

A second pathway leading to an NO^+-like species would be catalysis of $^{\bullet}NO$ oxidation by an oxidized transition metal complex as present in nitroprusside $(Fe(III)NO(CN)_5)^{2-}$. This would require continuous reoxidation of the reduced metal ion. Indeed, metal-based mechanisms for nitros(yl)ation were previously proposed [26,27].

More recently a third pathway was suggested when indirect evidence indicated an interaction of $^{\bullet}NO$ with peroxynitrous acid [16,28,29], which owing to its pK_a value of 6.6, is in equilibrium with peroxynitrite [30]. According to the reaction

$$^{\bullet}NO + HOONO \rightarrow NO_2^- + H^+ + {}^{\bullet}NO_2 \quad (4)$$

the $^{\bullet}NO_2$ radical could yield N_2O_3 with an additional molecule of $^{\bullet}NO$, resulting eventually in a stoichiometry of 3 $^{\bullet}NO$ to 1 $^{\bullet}O_2^-$ for the nitros(yl)ation process via N_2O_3. If the above reaction would be sufficiently fast, a low steady-state level of peroxynitrite would be the consequence in the presence of an excess of $^{\bullet}NO$. This was experimentally supported by complete abolishment of the peroxynitrite mediated zinc finger oxidation in alcohol dehydrogenase at an about threefold molar excess of $^{\bullet}NO$ over $^{\bullet}O_2^-$ [29]. Superoxide fluxes were generated by hypoxanthine/xanthine oxidase (HX/XO) and $^{\bullet}NO$ fluxes by spermine NONOate (SPENO). Whereas Espey *et al.* [16] observed an optimum of diaminonaphthalene (DAN) nitrosation also at a ratio of 3 $^{\bullet}NO$: 1$^{\bullet}O_2^-$, we had reported nitrosation of phenol by coincubating equimolar concentrations of 3-morpholinosydnonimine hydrochloride (Sin-1) and SPENO [29]. The aerobic thermal decomposition of Sin-1 releases $^{\bullet}NO$ and $^{\bullet}O_2^-$ at equal rates [31] and SPENO generates 2 mol of $^{\bullet}NO$ [32] thus resulting in a stoichiometric release of 3 $^{\bullet}NO$ and 1 $^{\bullet}O_2^-$. This system yielded fivefold higher amounts of 4-nitrosophenol compared to Sin-1 and SPENO alone [29]. To address the underlying mechanism in detail we here used the methodology and the concept of two papers published in 2002 [16,29].

Precise kinetics of the decay curves, however, were not considered in these previous publications. In such complex systems, secondary reactions of NONOate with $^{\bullet}O_2^-$ or peroxynitrite could arise, or the kinetics of $^{\bullet}O_2^-$ generation by xanthine oxidase could have been modified by reactive intermediates. In addition, because peroxynitrite at pH 12 did not react with $^{\bullet}NO$, the reaction of $^{\bullet}NO$ with peroxynitrous acid (Eq. 4) also has been seriously questioned [33].

To highlight the biological significance of the herein described nitros(yl)ation mechanism, $NADP^+$-dependent isocitrate dehydrogenase (ICDH) was chosen as a biologically relevant target, because its *S*-nitros(yl)ation had been shown to inhibit the enzyme [34,35]. However, it should be noted that purified enzymes are only part of a biological model because the complex environment of the cell is only partially mimicked [36].

As a new nitros(yl)ation model we here propose the aerobic decay of Sin-1 in the presence of Cu,Zn-superoxide dismutase (Cu,Zn-SOD), which was suited to display *S*-nitros(yl)ation of ICDH at a defined maximum without considerable S-NO formation by peroxynitrite or $^{\bullet}NO$ alone. This system has the potential to serve as a suitable model to study cellular *S*-nitros(yl)ation reactions under kinetically identical flux conditions for $^{\bullet}NO$ and $^{\bullet}O_2^-$.

Materials and Methods

Materials

Sin-1 was obtained from Calbiochem (La Jolla, CA, USA). SPENO was purchased from Cayman Chemicals (Ann Arbor, MI, USA), DAN and dihydrorhodamine 123 (DHR) were from Fluka (Buchs, Switzerland). Polyethylene-glycolated Cu,Zn-superoxide dismutase (PEG-SOD; EC 1.15.1.1) from bovine erythrocytes, $NADP^+$-dependent ICDH (EC 1.1.1.42) type IV from porcine heart (solution in 50% glycerol), XO (EC 1.1.3.22) grade III from buttermilk, cytochrome c, *S*-nitrosoglutathione, and 4-nitrosophenol were provided by Sigma-Aldrich (Deisenhofen, Germany).

N-nitrosation

A solution of DAN (2.5, 20, or 100 μM) in potassium phosphate buffer (0.1 M, pH 7.4) was incubated with a fixed concentration of Sin-1 (1, 10, or 100 μM) in the presence of increasing amounts of SPENO (0.1-1000 μM) for 90 min at 37°C. $^{\bullet}NO$-alone control was performed with 20 μM DAN and SPENO (1-100 μM) without Sin-1. DAN *N*-nitrosation (triazol formation) was measured by fluorescence detection (excitation 370 nm; emission 460 nm) using a Twinkle fluorescence plate reader (Berthold Technologies, Bad Wildbad, Germany). Similar experiments were performed with a solution of DAN (20 or 100 μM) and a fixed concentration of Sin-1 (10 or 100 μM) in the presence of increasing amounts of PEG-SOD (0.00033-100 U/ml) for 90 min at 37°C. $^{\bullet}NO$ alone control was performed with 20 μM DAN and 10 μM SPENO with PEG-SOD (0.00033-100 U/ml). The effect of bicarbonate (25 mM) on *N*-nitrosation was studied in a system with 20 μM DAN, 10 μM Sin-1, and PEG-SOD (0.00033-100 U/ml). The concentration-dependent effects of bicarbonate (0.001-100 mM), uric acid (0.0001-10 mM), and sodium azide (0.001-100 mM) were tested under maximal nitrosation conditions in the presence of 100 μM Sin-1 and 3.3 U/ml PEG-SOD at pH 7.4 (the pH was controlled and adjusted where necessary).

Dihydrorhodamine 123 oxidation

The kinetics of peroxynitrite (from Sin-1; 10 or 100 μM)-dependent oxidation of DHR (50 μM) were determined by fluorescence detection (ex 500 nm, em 535 nm) over 90 min using

a Twinkle fluorescence plate reader. The decrease in DHR oxidation was measured as a function of the PEG-SOD concentration (0.00033-333 U/ml).

•NO release from Sin-1 and SPENO

•NO release from Sin-1 (10 or 100 μM) was qualitatively assessed in the presence of PEG-SOD (1-100 U/ml) using an •NO electrode (Ami NO-700, Innovative Instruments, Quee Brooks Court, FL, USA). The electrode was calibrated daily with $NaNO_2$ standards in 0.1 M H_2SO_4 containing 100 μM potassium iodide. For calibration of the instrument, the Δ-current between the baseline and the peak after addition of $NaNO_2$ was determined. Additionally, •NO release from SPENO (10-30 μM) was quantitatively assessed using the oxidation of oxyHb to metHb as previously published [37].

SOD activity assay and cytochrome c-dependent determination of superoxide formation rates

PEG-SOD (Sigma) in 100 mM potassium phosphate, pH 7.4, was incubated with Sin-1 or SPENO at 37°C for 5 h to allow complete decomposition of the compounds. PEG-SOD (2.5 U/ml) was then added to a system containing 50 mU/ml xanthine oxidase (Fluka), 1 mM hypoxanthine (LKT Laboratories), and 50 μM cytochrome c (Sigma). The reduction of cytochrome c was measured at 550 nm over a period of 3 min [8,37]. Superoxide formation rates were measured in the absence of SOD with XO (0.1-10 mU/ml) by reduction of cytochrome c at 550 nm using $\varepsilon_{550} = 19.5\ mM^{-1}\ cm^{-1}$ as previously published [37].

C-nitrosation

A solution of phenol (5 mM) in potassium phosphate buffer (0.1 M, pH 7.4) was incubated with a fixed concentration of Sin-1 (20 μM) in the presence of increasing amounts of PEG-SOD (0.1-2500 U/ml) for 90 min at 37°C. Similar experiments were performed with 10 mM phenol and 200 μM Sin-1 and PEG-SOD (0.1-2500 U/ml). In another set of experiments, a solution of phenol (5 mM) in potassium phosphate buffer (0.1 M, pH 7.4) was incubated with a fixed concentration of Sin-1 (10 μM) in the presence of increasing amounts of SPENO (2.5-100 μM) for 90 min at 37°C. •NO alone controls were also performed. The concentration-dependent effects of bicarbonate (0.001-100 mM), uric acid (0.0001-10 mM), and sodium azide (0.001-100 mM) were tested under maximal *C*-nitrosation conditions in the presence of 5 mM phenol, 20 μM Sin-1, and 33 U/ml PEG-SOD at pH 7.4 (the pH was controlled and adjusted when necessary). Phenol *C*-nitrosation (4-nitrosophenol formation) was measured by HPLC. Briefly, the samples were kept on ice and 100 μl was subjected to HPLC analysis using an M480 HPLC pump and SP-6 UV–Vis spectrophotometric detector from Gynkotek GmbH (Germering, Germany) and a ChromJet integrator from Thermo Separation Products (Hertfordshire, UK). The main product, 4-nitrosophenol, was isocratically eluted (0.8 ml/min flow) using a C_{18}-Nucleosil 125×4 100-3 reversed-phase column from Macherey-Nagel GmbH (Düren, Germany). The mobile phase contained acetonitrile (35%) in 50 mM citric acid buffer (65%), pH 2.2. Nitrosophenol was detected at 300 nm and quantified using an internal and external standard (4-nitrosophenol). The typical retention time was 2.5 min.

S-nitros(yl)ation

A solution of ICDH (5 μM) in potassium phosphate buffer (0.1 M, pH 7.4) was incubated with a fixed concentration of Sin-1 (30 μM) in the presence of increasing amounts of SPENO (0.033-1000 μM) for 90 min at 37°C. Identical experiments were performed with increasing amounts of PEG-SOD (0.001-333 U/ml) instead of SPENO. Qualitatively similar results were obtained when a mixture of ICDH (1 μM) and Sin-1 (50 μM) was incubated for 90 min at 37°C in the presence of increasing amounts of PEG-SOD (0.033-333 U/ml). *S*-nitros(yl)ation of ICDH (*S*-nitrosocysteine formation) was detected by dot blot analysis using a specific antibody against *S*-nitrosocysteine. Briefly, 20 μl (for 5 μM ICDH) or 100 μl (for 1 μM ICDH) of each sample (approximately 75 μg of protein) was transferred to a Protran BA85 (0.45-μm) nitrocellulose membrane (Schleicher & Schuell, Dassel, Germany) by a Minifold I vacuum dot-blot system (Schleicher & Schuell, Dassel, Germany). Each slot was washed with 250 μl PBS and the membrane was dried for 15 min at 60°C. For detection of *S*-nitros(yl)ated protein, a rabbit polyclonal nitrosocysteinyl-residue antibody (Alexis, San Diego, CA, USA) was used at a dilution of 1:1000. Positive dots were detected by enhanced chemiluminescence after incubation with a peroxidase-coupled secondary antibody (GAR-POX, 1:5000) (Vector Laboratories, Burlingame, CA, USA). All incubation and washing steps were performed according to the manufacturer's instructions. Densitometric quantification was performed by using a high-resolution scanner (Biometra/Epson) equipped with the densitometry software Gel Pro Analyzer (Media Cybernetics, Bethesda, MD, USA). Specificity of the antibody used was tested by decomposition of *S*-nitrosocysteine by addition of 10 mM dithiothreitol (DTT) or 100 μM $HgCl_2$ to an SNO-positive ICDH sample 10 min before the transfer to the membrane. *S*-nitros(yl)ation of ICDH was also detected by trace metal-driven decomposition and subsequent DAN-dependent fluorescence. Briefly, 2.5 μM ICDH was incubated for 120 min without or with 50 μM Sin-1 plus 0.1, 3.3, or 100 U/ml PEG-SOD. After dilution 1:4 with buffer approximately 80% of the volume was removed by size exclusion centrifugation using a 10-kDa Microcon filter device (Millipore, Bedford, MA, USA). The remaining 20% was diluted 1:4 with buffer and these steps were repeated a third time, resulting in a more than 100-fold dilution of the reaction solution. These steps were performed to remove nitrite and other Sin-1 decomposition products, which could lead to false-positive results. The final sample in the filter containing the ICDH but almost no Sin-1 products was mixed 1:1 with DAN (50 μM), $HgCl_2$ and $CuSO_4$ were added (25 μM each). The DAN fluorescence was measured using a Twinkle fluorescence plate reader before and 20 min after addition of trace metals. The values without trace metals were subtracted from those with copper and mercury. *S*-nitros(yl)ation was also assessed by GSNO formation. GSH (1 mM) was incubated with 20 μM Sin-1 and increasing concentrations of PEG-SOD (0.1–333 U/ml) for 90 min at 37°C in 0.1 M potassium phosphate buffer, pH 7.4. GSNO formation was quantified by an HPLC-based method using an ion-exchange column, Nucleosil 100-5SA, 150×4.6 mm, with a mobile phase of 4.5 g/L ammonium citrate and 6 g/L phosphoric acid in water (pH 2.2). The flow rate was 1 ml/min. The optical detection of GSNO at 338 nm resulted in a limit of quantification of GSNO at 0.1 μM.

Results

Reactants for chemical nitros(yl)ation models

The three reactants used are depicted in Fig. 1 and have been employed in the model systems. More detailed considerations on the use of these reactants and their nitros(yl)ation mechanisms are provided in the online supplementary materials.

The hypoxanthine/xanthine oxidase/spermine NONOate system

Fluxes of $^{\bullet}O_2^-$ can be conveniently generated by the HX/XO reaction and can be quantified by the reduction of cytochrome c [37]. It is also practical to use NONOates as sources for continuous $^{\bullet}NO$ generation, which can be monitored polarographically, and because they are available with various half-lives for their thermal decay under release of one or two molecules of $^{\bullet}NO$, a close match to the kinetics of $^{\bullet}O_2^-$ formation can be achieved. This setup with SPENO as the $^{\bullet}NO$ donor has been used by us [24,29] and others [16,38] to study the formation and fate of peroxynitrite with a concomitant generation of nitrosating intermediates.

It was also difficult to meet the argument that the rates could be the subject of modulation by the reactive intermediates generated. Likewise, xanthine oxidase is inhibited by peroxynitrite [39,40] and its SH groups may also be targets for nitrosating species [41], although we observed no significant loss of XO activity in response to incubation with Sin-1 (Supplementary Fig. 1S). In addition, uric acid as a potential product of hypoxanthine oxidation may trap $^{\bullet}NO_2$ or peroxynitrite [42,43]. Similarly, NONOates may be influenced in their decay by the simultaneous presence of $^{\bullet}O_2^-$ or by radicals derived from peroxynitrite, and vice versa, the release of $^{\bullet}O_2^-$ by XO may change in the presence of $^{\bullet}NO$.

As a first approach we repeated the nitrosation of DAN in the system HX/XO/SPENO with a short incubation time of only 5 min, for which an almost linear formation of $^{\bullet}NO$ and $^{\bullet}O_2^-$ could be assumed (Fig. 2). Under such conditions, increasing concentrations of XO with a fixed amount of hypoxanthine and SPENO resulted in a maximum for the nitrosation of DAN (Fig 2). The measured rates of $^{\bullet}NO$ and $^{\bullet}O_2^-$ formation from 30 μM SPENO and 0.33 mU/ml XO were 735 ± 29 and 128 ± 14 nM/min, respectively. In accordance, the ratio at the nitrosation maximum in Fig. 2A was 5.74 $^{\bullet}NO$:1 $^{\bullet}O_2^-$. At the maximum in Fig. 2B (10 μM SPENO and 0.21 mU/ml XO) the calculated ratio was 3.02 $^{\bullet}NO$:1 $^{\bullet}O_2^-$. The measured formation rates were in good accordance with previous literature data (see extended results in the supplementary material).

The Sin-1/spermine NONOate system

As a second approach, we replaced the supposedly vulnerable $^{\bullet}O_2^-$ generation of the HX/XO system by a chemical $^{\bullet}O_2^-$ source. Sin-1 in aerated aqueous solutions at pH 7.4 generates equimolar fluxes of $^{\bullet}NO$ and $^{\bullet}O_2^-$ with a reported half-life of about 35 min [44]. According to our own measurements based on DHR oxidation, the half-life under the present conditions (100 mM potassium phosphate buffer, 37°C, pH 7.4) was 40 min (not shown). For the half-life of SPENO measured under our assay conditions by a polarographic $^{\bullet}NO$ detection, about 40 min was also established, in accordance with

previous reports [32]. Both compounds decayed by first-order kinetics with therefore very similar half-lives, suggesting that a 1:1 aerobic mixture should result in •NO: $•O_2^-$ fluxes of approximately 3:1. Considering the necessity of dioxygen for $•O_2^-$ formation by Sin-1 at a concentration of 30 μM, an air-saturated buffer system (O_2 240 μM) was used to guarantee dioxygen saturation. Under these conditions we had found a fivefold higher phenol nitrosation compared with the two components alone [29] after an incubation time of 90 min, during which both donors would have decomposed by first-order kinetics. Because no variation in the flux rates was performed in the previous experiment we now have repeated such data, but with DAN as a reactant.

Using Sin-1 as low as 1 μM, the addition of increasing amounts of SPENO led to a maximum at about 1.0 μM SPENO, with a decrease at 2 μM, after which a higher level was maintained up to 10 μM SPENO (Fig. 3A). With 10 μM Sin-1 (Fig. 3B) a maximum was found at about 12 μM SPENO with a decline at 30 μM followed by a steady increase up to 100 μM. With 100 μM SPENO (Fig. 3C), a maximum was hardly visible at about 120 μM and the reaction proceeded linearly from about 200 μM on. Controls with NONOate alone were run for the 100 μM concentration range showing a rather linear increase in DAN nitrosation (Fig. 3B).

Thus, at all three concentrations of Sin-1, maxima were observed at about equimolar SPENO and Sin-1 concentrations leading to a calculated ratio of about 3:1 with 1 μM Sin-1 or about 3.4:1 •NO over $•O_2^-$ with 10 and 100 μM Sin-1.

The data clearly indicate that with •NO alone under aerobic conditions DAN undergoes nitrosation. However, the presence of $•O_2^-$ enhances this basal activity, leading to the observed maxima. It is evident that a subtraction of the basal activity is not justified because the presence of $•O_2^-$ will interfere with the concentration of •NO at the maximum of nitrosation. It is also evident that at higher concentrations of •NO (>100 μM) the autoxidation of •NO becomes an appreciable source of DAN nitrosation covering the maximum observed at more physiological flux rates of 3 •NO :1 $•O_2^-$ (Fig. 3C).

The Sin-1/Cu,Zn-SOD system

Given the thermal decomposition of Sin-1 into •NO and the oxidation of the resulting radical by dioxygen to $•O_2^-$, it should be possible to dismutate the resulting $•O_2^-$ by SOD to shift the •NO:$•O_2^-$ ratio from 1:1 to higher values. Taking into account the extremely fast reaction of •NO with $•O_2^-$, the competing concentrations of SOD should be high to achieve this effect. Manganese SOD is known to be nitrated and inactivated by peroxynitrite [3] and hence could not be used. Cu,Zn-SOD also can be inhibited by peroxides but in a reversible manner [45]. Indeed, Cu,Zn-SOD at rather low levels has been shown to be pronitrosative in the presence of Sin-1 [46]. Using the polarographic detection of •NO by a selective •NO electrode [47], it was possible to detect •NO in Sin-1 incubations upon addition of increasing concentrations of Cu,Zn-SOD (not shown). Because polyethylene-glycolated Cu,Zn-SOD is considered to be more stable, this derivative was used further on and very similar results were obtained (Fig 4A). The detection of •NO required a lag phase of about 25 s and then increased with time. Interestingly, after about 3 min the lower concentrations of 1, 5, and 10 U/ml led to a plateau indicating a steady-state level of •NO, whereas higher concentrations

of 50 and 100 U/ml caused a sustained increase over at least 10 min (Fig. 4A). This proves that Cu,Zn-SOD can effectively compete with •NO and thus prevent $•O_2^-$ from combining with •NO, but also indicates that at low concentrations, leaving sufficient $•O_2^-$ for peroxynitrite formation, •NO is consumed in the system and stays at a low steady-state level. Further support for trapping $•O_2^-$ by Cu,Zn-SOD during Sin-1 decay came from measurements of DHR oxidation, which has been used to monitor peroxynitrite [48] (Fig 4B). High concentrations of Cu,Zn-SOD could largely block this oxidation but already low concentrations up to 10 U/ml abolished about 50% of the oxidation rate. Under these conditions the effects of Cu,Zn-SOD on the nitrosation were investigated. At concentrations of 10 μM DAN and 10 μM Sin-1, the nitrosation reached a maximum at about 10 U/ml Cu,Zn-SOD and returned almost back to the baseline at 100 U/ml (Fig. 4C). Fig. 4D provides all three parameters (•NO release, DHR oxidation, and DAN nitrosation) as a function of PEG-SOD concentration at 40 min incubation time.

C-nitrosation of phenol and S-nitros(yl)ation of ICDH and glutathione in the Sin-1 systems

The two new model systems for nitros(yl)ation, in which the kinetic disadvantages of the HX/XO–SPENO system were largely eliminated, were used for the *C*-nitrosation of phenol and for the *S*-nitros(yl)ation of the reactant ICDH in further experiments. The nitrosation maximum for phenol in the Sin-1 (20 μM)/SPENO (20 μM) system was less pronounced than that for the *N*-nitrosation of DAN. However, an intermediary plateau was reached, which was absent in the control with •NO alone, at a level four- to fivefold higher than with SPENO or Sin-1 alone (Fig. 5A). The generation of a nitrosating species peaked similar to DAN at a ratio of approximately 3 •NO to 1 $•O_2^-$. Considerable amounts of 4-nitrosophenol seemed to be formed via •NO autoxidation indicating an $•O_2^-$ independent nitrosation process under aerobic conditions. It should be taken into account that •NO accumulates under these conditions and then reaches sufficient concentrations for its autoxidation with dioxygen. In the system Sin-1/PEG-SOD, 20 μM Sin-1 was used and about 33 U/ml SOD was needed to obtain the maximum in phenol nitrosation (Fig. 5B). It should be noted that a higher PEG-SOD/Sin-1 ratio was required to reach the phenol nitrosation maximum compared to DAN and ICDH nitros(yl)ation. This could be related to the formation of phenoxy radicals as intermediates giving rise to the contribution of a radical-based mechanism in the case of phenol. Interestingly, the formation of 4-nitrophenol was detectable only in controls (Sin-1 alone; not shown) and up to 1 U/ml SOD (Fig. 5C, inset), suggesting that peroxynitrite was indeed consumed to yield a nitrosating species at concentrations of SOD in the range of 10-30 U/ml.

Clearly defined results were obtained with ICDH as a reactant (Fig. 6A). The dot-blot for the *S*-nitros(yl)ated enzyme showed a distinct optimum at 35 μM SPENO at a Sin-1 concentration of 30 μM, which is in good agreement with the data on DAN. The calculated ratio for $•NO:•O_2^-$ reached a value of about 3:1.

A very similar bell-shaped curve was obtained for the *S*-nitros(yl)ation of the ICDH in the system Sin-1/SOD. The optimum occurred at about 3.3 mU/ml PEG-SOD, with the remarkable observation of absence of any *S*-nitros(yl)ation at very low as well as at high levels of SOD (Fig 6B). High concentrations of DTT and micromolar amounts of $HgCl_2$

could efficiently decrease the SNO-positive signal, suggesting good specificity of the antibody (Fig. 6C). Additional support came from direct measurement of SNO groups in ICDH by trace metal triggered decomposition and DAN fluorescence, which was maximal upon treatment of the enzyme with 3.3 U/ml PEG-SOD and 50 μM Sin-1 (Fig. 6D). Obviously neither peroxynitrite nor •NO alone was very effective in this process. We also verified that Cu,Zn-SOD was not inactivated over the course of Sin-1 or SPENO incubations (Supplementary Fig. 2S). Importantly, the SOD-derived maximum in nitrosation and also the concentration-dependent increase in •NO formation were mimicked by the SOD-mimetic $Cu(II)_2(3,5\text{-diisopropylsalicylate})_4$ at catalytic concentrations (Supplementary Fig. 3S). Because glutathione is the most abundant cellular thiol compound and to provide further evidence for a biological role of the herein described nitros(yl)ation mechanism, we investigated GSNO formation as a function of the $•NO/•O_2^-$ ratio. The Sin-1/PEG-SOD system showed a clear maximum at 33 U/ml PEG-SOD (Fig. 6E, Supplementary Fig. 6S).

Discussion

Chemical model systems can be useful for studying biologically relevant mechanisms without interference by other cellular components. A suitable example in this respect turned out to be the *S*-nitros(yl)ation of purified enzymes, whereas the chemical reactants DAN and phenol seemed to be nitrosated by more than one mechanism and hence were of only limited value as model substrates. We here suggest that at physiologically low levels of •NO, in the nanomolar range, the reaction of two molecules of •NO with dioxygen, resulting in $•NO_2$ as an intermediate for nitros(yl)ation mechanisms via thiyl radicals or N_2O_3, becomes too slow because of the third-order kinetics involved. At nanomolar fluxes of •NO, derived from the thermal decomposition of SPENO, indeed, no significant *S*-nitros(yl)ation of ICDH could be detected. In contrast, simultaneous generation of $•O_2^-$ caused a dramatic rise in protein-bound *S*-nitroso groups, with a maximum at around 3 •NO:1 $•O_2^-$ as generated in the Sin-1/SPENO system (Fig. 3). A similar maximum of *S*-nitros(yl)ation was obtained in the Sin-1/PEG-SOD system with SOD activities that left an excess of •NO over peroxynitrite (Fig. 5). Sin-1 alone, generating low 1:1 fluxes of •NO and $•O_2^-$, leading to intermediate peroxynitrite formation, was not effective. Together, these results indicate that in our model systems *S*-nitros(yl)ation proceeds optimally at •NO : $•O_2^-$ fluxes at a ratio of 3:1, whereas peroxynitrite and aerobic •NO solutions are much less effective at the low fluxes employed.

Qualitatively, the occurrence of a nitrosating species at a 3:1 flux ratio could be confirmed by the use of phenol and DAN as reactants for *C*- and *N*-nitrosations, respectively. However, at variance with *S*-nitros(yl)ation of ICDH, the presence of •NO fluxes alone in aerobic solution already caused a basal nitros(yl)ation in absence of $•O_2^-$, suggesting that radical species such as $•NO_2$ or the peroxynitrite radical, •OONO, could be involved. With $•O_2^-$ present, however, the yields of nitros(yl)ation were greatly increased and this additional activity could be explained by a reaction of peroxynitrite/peroxynitrous acid with •NO. Because the peroxynitrite anion clearly does not react with •NO [33], the active species must be the acid form, which shows higher reactivity and tends to undergo homolytic cleavage at the O-O bond.

Results in the literature [48] are in support of this reaction and, from data by Crow and Beckman [28] as well as Schrammel *et al.* [21], even a high reaction rate can be deduced. Based on these observations one can conclude the following steps leading to N_2O_3 as a nitrosating species:

	$^{\bullet}NO + {}^{\bullet}O_2^-$	$ONOO^-$	(Eq. 5)
	$ONOO^- + H^+$	HOONO	(Eq. 6)
	$HOONO + {}^{\bullet}NO$	$[HO^-\cdots NO^+] + {}^{\bullet}NO_2$	(Eq. 7)
	$[HO^-\cdots NO^+]$	$NO_2^- + H^+$	(Eq. 8)
	$^{\bullet}NO_2 + {}^{\bullet}NO$	N_2O_3	(Eq. 9)
Sum	$3\ {}^{\bullet}NO + {}^{\bullet}O_2^-$	$N_2O_3 + NO_2^-$	(Eq. 10)

Thus, the generation of N_2O_3 from $^{\bullet}NO$ and $^{\bullet}O_2^-$ would consume 3 mol of $^{\bullet}NO$ and 1 mol of $^{\bullet}O_2^-$ (Eq. 10), in agreement with the stoichiometry obtained with the three reactants in the three model systems introduced in this work. However, it seems too early to postulate N_2O_3 as the only nitrosating species, because the oxidation of $^{\bullet}NO$ by peroxynitrous acid could generate an NO^+-like species as indicated in brackets (Eq. 7), which, despite its rapid reaction with OH^- (Eq. 8), could exist in a stabilized state over sufficient time to attack the nucleophilic centers at nitrogens, carbons, or sulfurs.

One could differentiate between both pathways by the use of azide (N_3^-) as a known inhibitor of N_2O_3 [49]. Indeed, phenol nitrosation in the Sin-1/SOD system was blocked with an IC_{50} of 100 μM azide but DAN nitrosation required about 10 mM azide (Supplementary Fig. 4S). This may not be taken as in favor or against N_2O_3 or the nitrosonium type mechanism, but may only be indicative of two mechanisms participating to variable extents with the two reactants. Supportive for this suggestion is that CO_2 in a bicarbonate buffer affects phenol nitrosation by a 50% increase, whereas for DAN, it is up to 400% higher at 100 mM (Supplementary Fig. 4S). Because CO_2 is known to stabilize peroxynitrite as an adduct [50], such results favor the involvement of peroxynitrite, but obviously to different extents with the two reactants. The possibility that $^{\bullet}NO$ could react only with the CO_2 adduct of peroxynitrite, giving rise to the nitrosating species (a mixed anhydride of carbonic acid and nitrous acid), was also considered, but elimination of CO_2 from the assays still resulted in the basal nitrosation rates. This is further supported by the varying effect of uric acid, a well-known scavenger of peroxynitrite and peroxynitrite-derived free radicals such as $^{\bullet}NO_2$. Surprisingly, *S*-nitros(yl)ation of ICDH was minimal with $^{\bullet}NO$ alone, although electron abstraction from a thiolate seems likely. Among two recent investigations on thiyl radical formation, one is not in support of a biological pathway via S-radicals [51], whereas the other provides data in favor of thiyl radical formation during *S*-nitros(yl)ation reactions [25]. The two herein newly described model systems provide optimal conditions for the elucidation of the biologically generated *S*-nitros(yl)ating species by avoiding thiyl radical intermediates. Under very special conditions, a radical-based *S*-nitros(yl)ation involving thiyl radicals may take place and was recently reported to require electron transfer from a neighboring tyrosyl radical [52], which may have some impact for proteins with tyrosines and cysteines in close proximity [53]. It should be noted that the results with ICDH could be reproduced with glutathione, providing the basis for biological transnitrosation reactions.

There are further aspects in improving the above nitros(yl)ation models to approach physiological conditions. To suppress the radical pathways triggered by •NO autoxidation, the concentration of dioxygen should be lowered because the autoxidation of •NO occurs proportional to the O_2 partial pressure, whereas the reaction of the Sin-1 radical with dioxygen has a high reaction rate and should be saturated already at low oxygen concentrations. Special emphasis should also be put on the concentrations of •NO. Lowering its concentration will have a large suppressing effect on the radical oxidation pathway because it proceeds in a second-order reaction with respect to •NO. As can be deduced from the data in Fig. 3A, 1 μM Sin-1 shows the most pronounced maximum in DAN nitrosation, whereas at higher concentrations the autoxidation mechanism becomes more significant. Thus, it seems essential to set up the herein proposed model systems with low •NO fluxes under low dioxygen partial pressure in accordance with the physiological situation. Under cellular conditions the O_2 effect would be smaller and DAN and phenol nitrosation would be diminished. It can be calculated that 1-10 μM Sin-1 forms steady-state levels of •NO in the low nanomolar range, which closely mimics the situation in the cell.

Biological relevance of different nitros(yl)ation pathways

As outlined above, the flux rates for •NO and $•O_2^-$ generation under cellular conditions are low and hence favor a mechanism via peroxynitrite and its reaction with •NO versus the autoxidation of •NO. We are not excluding the autoxidation pathway nor the metal catalyzed oxidation of •NO or a tyrosyl radical-mediated formation of thiyls and their addition of •NO. However, in view of the extraordinary nucleophilicity of the thiolate group, a polar mechanism with the described characteristics seems more likely. Although the high pK value of GSH is not in favor of a high reaction rate, its concentration between 5 and 10 mM renders it a good NO^+ acceptor, in agreement with the occurrence of GSNO in various cells under oxidative stress [13]. Thus low pK thiolate groups of enzymes can either directly combine with the NO^+-like species or become nitros-(yl)ated by transnitrosation from GSNO. Selectivity for thiol groups seems to be associated with the nucleophilic properties of the sulfur, which does not exclude reactions with the less nucleophilic nitrogen atoms, explaining the occurrence of *N*-nitroso compounds *in vivo* [16–19]. One of the surprising results with ICDH and the new nitrosation model was the lack of nitrosation by •NO and peroxynitrite alone. With increasing $•O_2^-$ release in the presence of •NO, a maximum was reached, and by comparison with the Sin-1/SPENO system this occurred at •NO/$•O_2^-$ fluxes of about 3:1. A scenario to which this situation applies can be found for lipopolysaccharide (LPS; endotoxin)-stimulated macrophages, which produce •NO from inducible NOS-2 and $•O_2^-$ from activated NADPH oxidase, which has been previously demonstrated by Espey *et al.* in LPS/IFN-γ-stimulated murine ANA-1 macrophages [16]. The cellular relevance of these findings was further supported by *S*-nitros(yl)ation found in human MCF-7 breast carcinoma cells upon incubation with SPENO and XO. Moreover, the *S*-nitros(yl)ation and inhibition of glyceraldehyde-3-phosphate dehydrogenase under such conditions has been reported [54,55]. Similarly, a NOS-1-dependent SNO formation together with protein tyrosine nitration increase was found in PC12 cells after exposure to nerve growth factor (indicating •NO and peroxynitrite generation), but here the source of $•O_2^-$ was not yet identified [13,56]. Because •NO can block cytochrome c oxidase, an increased electron leak in the respiratory chain could provide $•O_2^-$ for this abundance of

SNO immunoreactivity. A last hypothetical scenario could be a pharmacological one: chronic treatment with nitroglycerin results in the development of nitrate tolerance, which is associated with protein tyrosine nitration [57], but acute nitroglycerin administration also lead to a dramatic increase in nitros(yl)ation of blood and tissue constituents [58]. Therefore, it may be expected that treatment of cells or tissue with nitroglycerin would be a good model for peroxynitrite driven nitros(yl)ation reactions. In contrast to our present findings a recent report by Lancaster and co-workers demonstrated the importance of dinitrosyl complexes for *S*-nitros(yl)ation in RAW 264.7 cells [59]. Although these authors did not report on bell-shaped *S*-nitros(yl)ation patterns, they showed a shoulder in the RSNO formation–DMNQ induced ROS generation relationship (their Fig. 4) indicating the participation of at least two distinct processes.

Conclusions

In summary, our results indicate that biological *S*-nitros(yl)ation may involve the formation of peroxynitrous acid, and its reaction with an excess of $^{\bullet}NO$ could give rise to N_2O_3 and/or a nitrosonium-like species. Owing to the low radical fluxes involved in an experimental system representing the cellular situation, neither phenol nor DAN turned out to be a suitable reactant for model investigations because they were also nitrosated by high $^{\bullet}NO$ fluxes alone, whereas enzymes with essential thiolate groups fulfill the requirements. Modulation of Sin-1-derived $^{\bullet}NO$ and $^{\bullet}O_2^-$ fluxes by $^{\bullet}NO$ and Cu,Zn-SOD seem to provide the closest conditions to study the mechanism of biological *S*-nitros(yl)ation processes. However, it should be noted that the systems used in this study are chemical models and require further proof for cellular relevance. Although the here-proposed nitros(yl)ation mechanism is chemically feasible and yielded maximal nitroso products in vitro, several mechanisms may contribute to the sum of nitros(yl)ations observed *in vivo*.

Supplementary Material

Refer to Web version on PubMed Central for supplementary material.

Acknowledgments

We thank Jörg Schreiner for expert technical assistance. This work was supported by generous financial support from the Johannes Gutenberg University and Hospital Mainz (MAIFOR and Forschungsfonds grants to A.D.) and the Robert Müller Foundation (stipend to J.M. and J.K.). M.M.B. was supported by the Whitaker Cardiovascular Institute and NIH grants R01 AG027080-04 and P01 HL081738-03. This paper contains results that are part of the doctoral thesis of Jens Kamuf.

References

1. Beckman JS, Koppenol WH. Nitric oxide, superoxide, and peroxynitrite: the good, the bad, and ugly. Am J Physiol. 1996; 271:C1424–37. [PubMed: 8944624]
2. Zou MH, Ullrich V. Peroxynitrite formed by simultaneous generation of nitric oxide and superoxide selectively inhibits bovine aortic prostacyclin synthase. FEBS Lett. 1996; 382:101–104. [PubMed: 8612727]
3. MacMillan-Crow LA, Crow JP, Kerby JD, Beckman JS, Thompson JA. Nitration and inactivation of manganese superoxide dismutase in chronic rejection of human renal allografts. Proc Natl Acad Sci U S A. 1996; 93:11853–11858. [PubMed: 8876227]

4. Hausladen A, Privalle CT, Keng T, DeAngelo J, Stamler JS. Nitrosative stress: activation of the transcription factor OxyR. Cell. 1996; 86:719–729. [PubMed: 8797819]
5. Whalen EJ, Foster MW, Matsumoto A, Ozawa K, Violin JD, Que LG, Nelson CD, Benhar M, Keys JR, Rockman HA, Koch WJ, Daaka Y, Lefkowitz RJ, Stamler JS. Regulation of beta-adrenergic receptor signaling by S-nitrosylation of G-protein-coupled receptor kinase 2. Cell. 2007; 129:511–522. [PubMed: 17482545]
6. Palmer LA, Doctor A, Chhabra P, Sheram ML, Laubach VE, Karlinsey MZ, Forbes MS, Macdonald T, Gaston B. S-nitrosothiols signal hypoxia-mimetic vascular pathology. J Clin Invest. 2007; 117:2592–2601. [PubMed: 17786245]
7. Mannick JB, Schonhoff C, Papeta N, Ghafourifar P, Szibor M, Fang K, Gaston B. S-Nitrosylation of mitochondrial caspases. J Cell Biol. 2001; 154:1111–1116. [PubMed: 11551979]
8. Frein D, Schildknecht S, Bachschmid M, Ullrich V. Redox regulation: a new challenge for pharmacology. Biochem Pharmacol. 2005; 70:811–823. [PubMed: 15899473]
9. Lipton SA, Choi YB, Pan ZH, Lei SZ, Chen HS, Sucher NJ, Loscalzo J, Singel DJ, Stamler JS. A redox-based mechanism for the neuroprotective and neurodestructive effects of nitric oxide and related nitroso-compounds. Nature. 1993; 364:626–632. [PubMed: 8394509]
10. Sumbayev VV, Budde A, Zhou J, Brüne B. HIF-1 alpha protein as a target for S-nitrosation. FEBS Lett. 2003; 535:106–112. [PubMed: 12560087]
11. Kelleher ZT, Matsumoto A, Stamler JS, Marshall HE. NOS2 regulation of NF-kappaB by S-nitrosylation of p65. J Biol Chem. 2007; 282:30667–30672. [PubMed: 17720813]
12. Foster MW, McMahon TJ, Stamler JS. S-nitrosylation in health and disease. Trends Mol Med. 2003; 9:160–168. [PubMed: 12727142]
13. Gow AJ, Chen Q, Hess DT, Day BJ, Ischiropoulos H, Stamler JS. Basal and stimulated protein S-nitrosylation in multiple cell types and tissues. J Biol Chem. 2002; 277:9637–9640. [PubMed: 11796706]
14. Hess DT, Matsumoto A, Kim SO, Marshall HE, Stamler JS. Protein S-nitrosylation: purview and parameters. Nat Rev Mol Cell Biol. 2005; 6:150–166. [PubMed: 15688001]
15. Chen Z, Foster MW, Zhang J, Mao L, Rockman HA, Kawamoto T, Kitagawa K, Nakayama KI, Hess DT, Stamler JS. An essential role for mitochondrial aldehyde dehydrogenase in nitroglycerin bioactivation. Proc Natl Acad Sci U S A. 2005; 102:12159–12164. [PubMed: 16103363]
16. Espey MG, Thomas DD, Miranda KM, Wink DA. Focusing of nitric oxide mediated nitrosation and oxidative nitrosylation as a consequence of reaction with superoxide. Proc Natl Acad Sci U S A. 2002; 99:11127–11132. [PubMed: 12177414]
17. Feelisch M, Rassaf T, Mnaimneh S, Singh N, Bryan NS, Jourd'Heuil D, Kelm M. Concomitant S-, N-, and heme-nitros(yl)ation in biological tissues and fluids: implications for the fate of NO in vivo. FASEB J. 2002; 16:1775–1785. [PubMed: 12409320]
18. Bryan NS, Rassaf T, Maloney RE, Rodriguez CM, Saijo F, Rodriguez JR, Feelisch M. Cellular targets and mechanisms of nitros(yl)ation: an insight into their nature and kinetics in vivo. Proc Natl Acad Sci U S A. 2004; 101:4308–4313. [PubMed: 15014175]
19. Simon DI, Mullins ME, Jia L, Gaston B, Singel DJ, Stamler JS. Polynitrosylated proteins: characterization, bioactivity, and functional consequences. Proc Natl Acad Sci U S A. 1996; 93:4736–4741. [PubMed: 8643472]
20. Ford PC, Wink DA, Stanbury DM. Autoxidation kinetics of aqueous nitric oxide. FEBS Lett. 1993; 326:1–3. [PubMed: 8325356]
21. Schrammel A, Gorren ACF, Schmidt K, Pfeiffer S, Mayer B. S-nitrosation of glutathione by nitric oxide, peroxynitrite, and (*)NO/O(2)(*-). Free Radic Biol Med. 2003; 34:1078–1088. [PubMed: 12684093]
22. Bonini MG, Augusto O. Carbon dioxide stimulates the production of thiyl, sulfinyl, and disulfide radical anion from thiol oxidation by peroxynitrite. J Biol Chem. 2001; 276:9749–9754. [PubMed: 11134018]
23. Bonini MG, Radi R, Ferrer-Sueta G, Ferreira AM, Augusto O. Direct EPR detection of the carbonate radical anion produced from peroxynitrite and carbon dioxide. J Biol Chem. 1999; 274:10802–10806. [PubMed: 10196155]

24. Daiber A, Bachschmid M, Beckman JS, Munzel T, Ullrich V. The impact of metal catalysis on protein tyrosine nitration by peroxynitrite. Biochem Biophys Res Commun. 2004; 317:873–881. [PubMed: 15081421]
25. Madej E, Folkes LK, Wardman P, Czapski G, Goldstein S. Thiyl radicals react with nitric oxide to form S-nitrosothiols with rate constants near the diffusion-controlled limit. Free Radic Biol Med. 2008; 44:2013–2018. [PubMed: 18381080]
26. Stubauer G, Giuffrè A, Sarti P. Mechanism of S-nitrosothiol formation and degradation mediated by copper ions. J Biol Chem. 1999; 274:28128–28133. [PubMed: 10497164]
27. Angelo M, Singel DJ, Stamler JS. An S-nitrosothiol (SNO) synthase function of hemoglobin that utilizes nitrite as a substrate. Proc Natl Acad Sci U S A. 2006; 103:8366–8371. [PubMed: 16717191]
28. Crow JP, Beckman JS. Reactions between nitric oxide, superoxide, and peroxynitrite: footprints of peroxynitrite in vivo. Adv Pharmacol. 1995; 34:17–43. [PubMed: 8562432]
29. Daiber A, Frein D, Namgaladze D, Ullrich V. Oxidation and nitrosation in the nitrogen monoxide/superoxide system. J Biol Chem. 2002; 277:11882–11888. [PubMed: 11805115]
30. Kissner R, Nauser T, Bugnon P, Lye P, Koppenol W. Formation and properties of peroxynitrite as studied by laser flash photolysis, high-pressure stopped-flow technique, and pulse radiolysis. Chem Res Toxicol. Nov; 1997 10(11):1285–1292. 11: 557; 1998. [PubMed: 9403183]
31. Feelisch M, Ostrowski J, Noack E. On the mechanism of NO release from sydnonimines. J Cardiovasc Pharmacol. 1989; 14 Suppl 1:S13–22. [PubMed: 2484692]
32. Maragos CM, Morley D, Wink DA, Dunams TM, Saavedra JE, Hoffman A, Bove AA, Isaac L, Hrabie JA, Keefer LK. Complexes of .NO with nucleophiles as agents for the controlled biological release of nitric oxide. Vasorelaxant effects. J Med Chem. 1991; 34:3242–3247. [PubMed: 1956043]
33. Goldstein S, Czapski G, Lind J, Merényi G. Effect of *NO on the decomposition of peroxynitrite: reaction of N2O3 with ONOO- Chem Res Toxicol. 1999; 12:132–136. [PubMed: 10027789]
34. Lee JH, Yang ES, Park JW. Inactivation of NADP+-dependent isocitrate dehydrogenase by peroxynitrite. Implications for cytotoxicity and alcohol-induced liver injury. J Biol Chem. 2003; 278:51360–51371. [PubMed: 14551203]
35. Yang ES, Richter C, Chun JS, Huh TL, Kang SS, Park JW. Inactivation of NADP(+)-dependent isocitrate dehydrogenase by nitric oxide. Free Radic Biol Med. 2002; 33:927–937. [PubMed: 12361803]
36. Lancaster JR, Gaston B. NO and nitrosothiols: spatial confinement and free diffusion. Am J Physiol Lung Cell Mol Physiol. 2004; 287:L465–6. [PubMed: 15308495]
37. Kelm M, Dahmann R, Wink D, Feelisch M. The nitric oxide/superoxide assay. Insights into the biological chemistry of the NO/O-2. interaction. J Biol Chem. 1997; 272:9922–9932. [PubMed: 9092531]
38. Jourd'heuil D, Miranda KM, Kim SM, Espey MG, Vodovotz Y, Laroux S, Mai CT, Miles AM, Grisham MB, Wink DA. The oxidative and nitrosative chemistry of the nitric oxide/superoxide reaction in the presence of bicarbonate. Arch Biochem Biophys. 1999; 365:92–100. [PubMed: 10222043]
39. Houston M, Chumley P, Radi R, Rubbo H, Freeman BA. Xanthine oxidase reaction with nitric oxide and peroxynitrite. Arch Biochem Biophys. 1998; 355:1–8. [PubMed: 9647660]
40. Lee CI, Liu X, Zweier JL. Regulation of xanthine oxidase by nitric oxide and peroxynitrite. J Biol Chem. 2000; 275:9369–9376. [PubMed: 10734080]
41. Ichimori K, Fukahori M, Nakazawa H, Okamoto K, Nishino T. Inhibition of xanthine oxidase and xanthine dehydrogenase by nitric oxide. Nitric oxide converts reduced xanthine-oxidizing enzymes into the desulfo-type inactive form. J Biol Chem. 1999; 274:7763–7768. [PubMed: 10075667]
42. Reiter CD, Teng RJ, Beckman JS. Superoxide reacts with nitric oxide to nitrate tyrosine at physiological pH via peroxynitrite. J Biol Chem. 2000; 275:32460–32466. [PubMed: 10906340]
43. Sawa T, Akaike T, Maeda H. Tyrosine nitration by peroxynitrite formed from nitric oxide and superoxide generated by xanthine oxidase. J Biol Chem. 2000; 275:32467–32474. [PubMed: 10906338]

44. Rosenkranz B, Winkelmann BR, Parnham MJ. Clinical pharmacokinetics of molsidomine. Clin Pharmacokinet. 1996; 30:372–384. [PubMed: 8743336]
45. Hodgson EK, Fridovich I. The interaction of bovine erythrocyte superoxide dismutase with hydrogen peroxide: inactivation of the enzyme. Biochemistry. 1975; 14:5294–5299. [PubMed: 49]
46. Hu TM, Hayton WL, Morse MA, Mallery SR. Dynamic and biphasic modulation of nitrosation reaction by superoxide dismutases. Biochem Biophys Res Commun. 2002; 295:1125–1134. [PubMed: 12135611]
47. Daiber A, Nauser T, Takaya N, Kudo T, Weber P, Hultschig C, Shoun H, Ullrich V. Isotope effects and intermediates in the reduction of NO by P450(NOR). J Inorg Biochem. 2002; 88:343–352. [PubMed: 11897349]
48. Jourd'heuil D, Jourd'heuil FL, Kutchukian PS, Musah RA, Wink DA, Grisham MB. Reaction of superoxide and nitric oxide with peroxynitrite. Implications for peroxynitrite-mediated oxidation reactions in vivo. J Biol Chem. 2001; 276:28799–28805. [PubMed: 11373284]
49. Caulfield JL, Wishnok JS, Tannenbaum SR. Nitric oxide-induced deamination of cytosine and guanine in deoxynucleosides and oligonucleotides. J Biol Chem. 1998; 273:12689–12695. [PubMed: 9582291]
50. Meli R, Nauser T, Latal P, Koppenol WH. Reaction of peroxynitrite with carbon dioxide: intermediates and determination of the yield of CO3*- and NO2*. J Biol Inorg Chem. 2002; 7:31–36. [PubMed: 11862538]
51. Hofstetter D, Nauser T, Koppenol WH. The glutathione thiyl radical does not react with nitrogen monoxide. Biochem Biophys Res Commun. 2007; 360:146–148. [PubMed: 17588542]
52. Zhang H, Xu Y, Joseph J, Kalyanaraman B. Intramolecular electron transfer between tyrosyl radical and cysteine residue inhibits tyrosine nitration and induces thiyl radical formation in model peptides treated with myeloperoxidase, H2O2, and NO2-: EPR SPIN trapping studies. J Biol Chem. 2005; 280:40684–40698. [PubMed: 16176930]
53. Foster MW, Stamler JS. New insights into protein S-nitrosylation. Mitochondria as a model system. J Biol Chem. 2004; 279:25891–25897. [PubMed: 15069080]
54. Molina y Vedia L, McDonald B, Reep B, Brüne B, Di Silvio M, Billiar TR, Lapetina EG. Nitric oxide-induced S-nitrosylation of glyceraldehyde-3-phosphate dehydrogenase inhibits enzymatic activity and increases endogenous ADP-ribosylation. J Biol Chem. 1992; 267:24929–24932. [PubMed: 1281150]
55. Hara MR, Agrawal N, Kim SF, Cascio MB, Fujimuro M, Ozeki Y, Takahashi M, Cheah JH, Tankou SK, Hester LD, Ferris CD, Hayward SD, Snyder SH, Sawa A. S-nitrosylated GAPDH initiates apoptotic cell death by nuclear translocation following Siah1 binding. Nat Cell Biol. 2005; 7:665–674. [PubMed: 15951807]
56. Cappelletti G, Maggioni MG, Tedeschi G, Maci R. Protein tyrosine nitration is triggered by nerve growth factor during neuronal differentiation of PC12 cells. Exp Cell Res. 2003; 288:9–20. [PubMed: 12878155]
57. Hink U, Oelze M, Kolb P, Bachschmid M, Zou MH, Daiber A, Mollnau H, August M, Baldus S, Tsilimingas N, Walter U, Ullrich V, Münzel T. Role for peroxynitrite in the inhibition of prostacyclin synthase in nitrate tolerance. J Am Coll Cardiol. 2003; 42:1826–1834. [PubMed: 14642695]
58. Janero DR, Bryan NS, Saijo F, Dhawan V, Schwalb DJ, Warren MC, Feelisch M. Differential nitros(yl)ation of blood and tissue constituents during glyceryl trinitrate biotransformation in vivo. Proc Natl Acad Sci U S A. 2004; 101:16958–16963. [PubMed: 15550545]
59. Bosworth CA, Toledo JC, Zmijewski JW, Li Q, Lancaster JR. Dinitrosyliron complexes and the mechanism(s) of cellular protein nitrosothiol formation from nitric oxide. Proc Natl Acad Sci U S A. 2009; 106:4671–4676. [PubMed: 19261856]

Abbreviations

Cu,Zn-SOD copper, zinc-superoxide dismutase

DAN	diaminonaphthalene
DHR	dihydrorhodamine 123
GSH	glutathione
GSNO	*S*-nitrosoglutathione
HX	hypoxanthine
ICDH	isocitrate dehydrogenase
PEG-SOD	polyethylene glycolated Cu,Zn-SOD
Sin-1	3-morpholino sydnonimine
SPENO	spermine NONOate
XO	xanthine oxidase

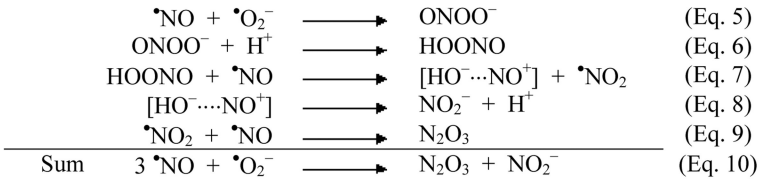

Eq. 5.

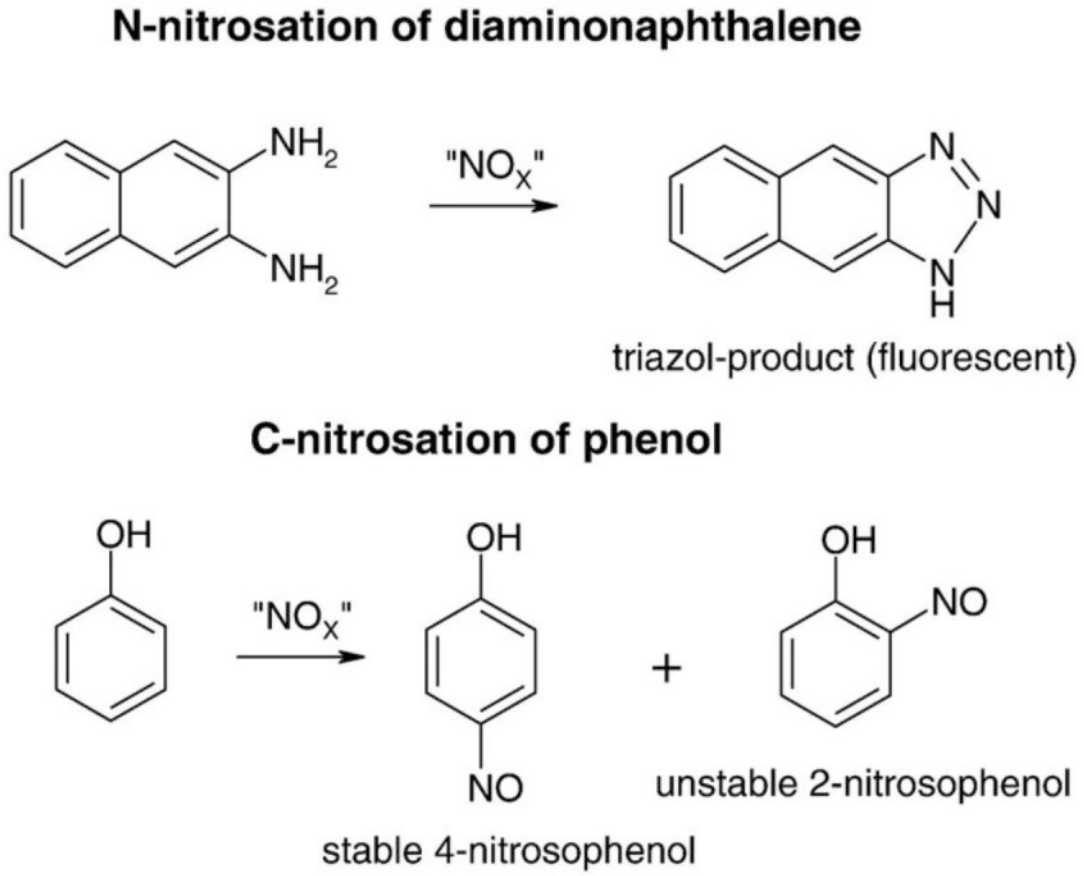

Fig. 1. Model systems for biological nitros(yl)ation reactions

For *N*-nitrosation the conversion of diaminonaphthalene to its highly fluorescent triazol product was used as a model. For *C*-nitrosation the formation of the stable 4-nitrosophenol product was monitored. For *S*-nitros(yl)ation the $NADP^+$-dependent isocitrate dehydrogenase (ICDH) was used as a reactant. The identity of the "NO_X" species is the subject of the Discussion.

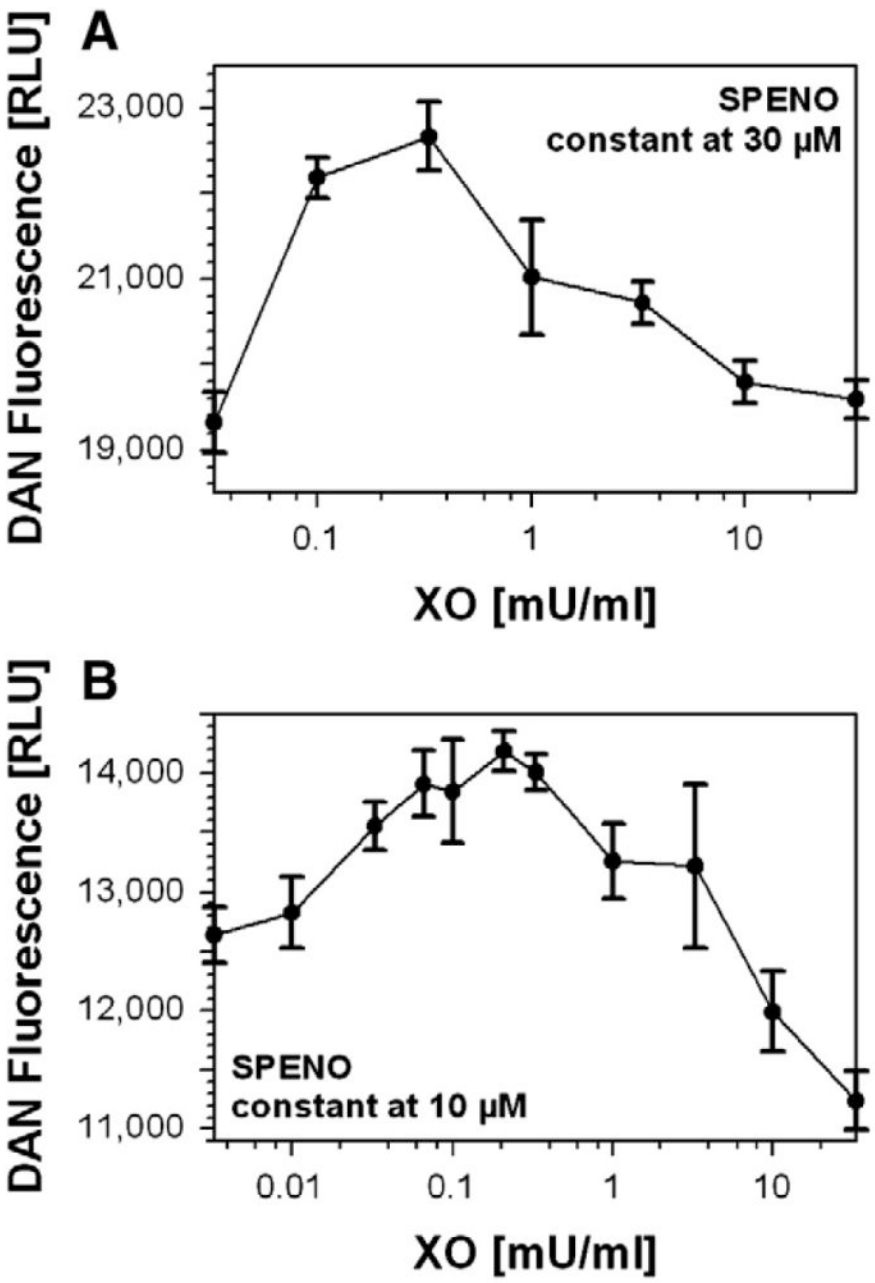

Fig. 2. *N*-nitrosation in the XO/HX/SPENO system

(**A**) DAN (100 µM) derived fluorescence was monitored at constant SPENO (30 µM) and increasing XO concentrations in 0.1 M potassium phosphate buffer, pH 7.4, containing 1 mM HX at 37°C. Data were collected after 5 min incubation. (**B**) DAN (20 µM) fluorescence was monitored at constant SPENO (10 µM) and increasing XO concentrations in 0.1 M potassium phosphate buffer, pH 7.4, containing 1 mM hypoxanthine at 37°C. Data were collected after 25 min incubation and are expressed as the means±SEM of two or three independent experiments.

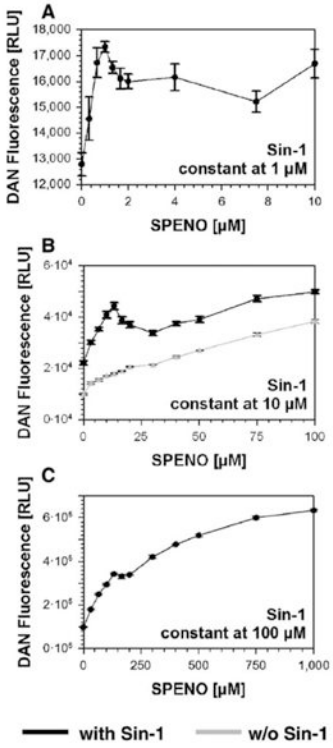

Fig. 3. *N*-nitrosation in the Sin-1/SPENO system

(**A**) DAN (2.5 µM) derived fluorescence was monitored at constant Sin-1 (1 µM) and increasing SPENO concentrations. (**B**) DAN (10 µM) fluorescence was monitored at constant Sin-1 (10 µM) and increasing SPENO concentrations. The effect of SPENO alone was tested in the absence of Sin-1 under similar conditions. (**C**) DAN (100 µM) fluorescence was monitored at constant Sin-1 (100 µM) and increasing SPENO concentrations. All experiments were performed in 0.1 M potassium phosphate buffer, pH 7.4, at 37°C and data were collected after 90 min incubation and expressed as the means±SEM of two or three independent experiments.

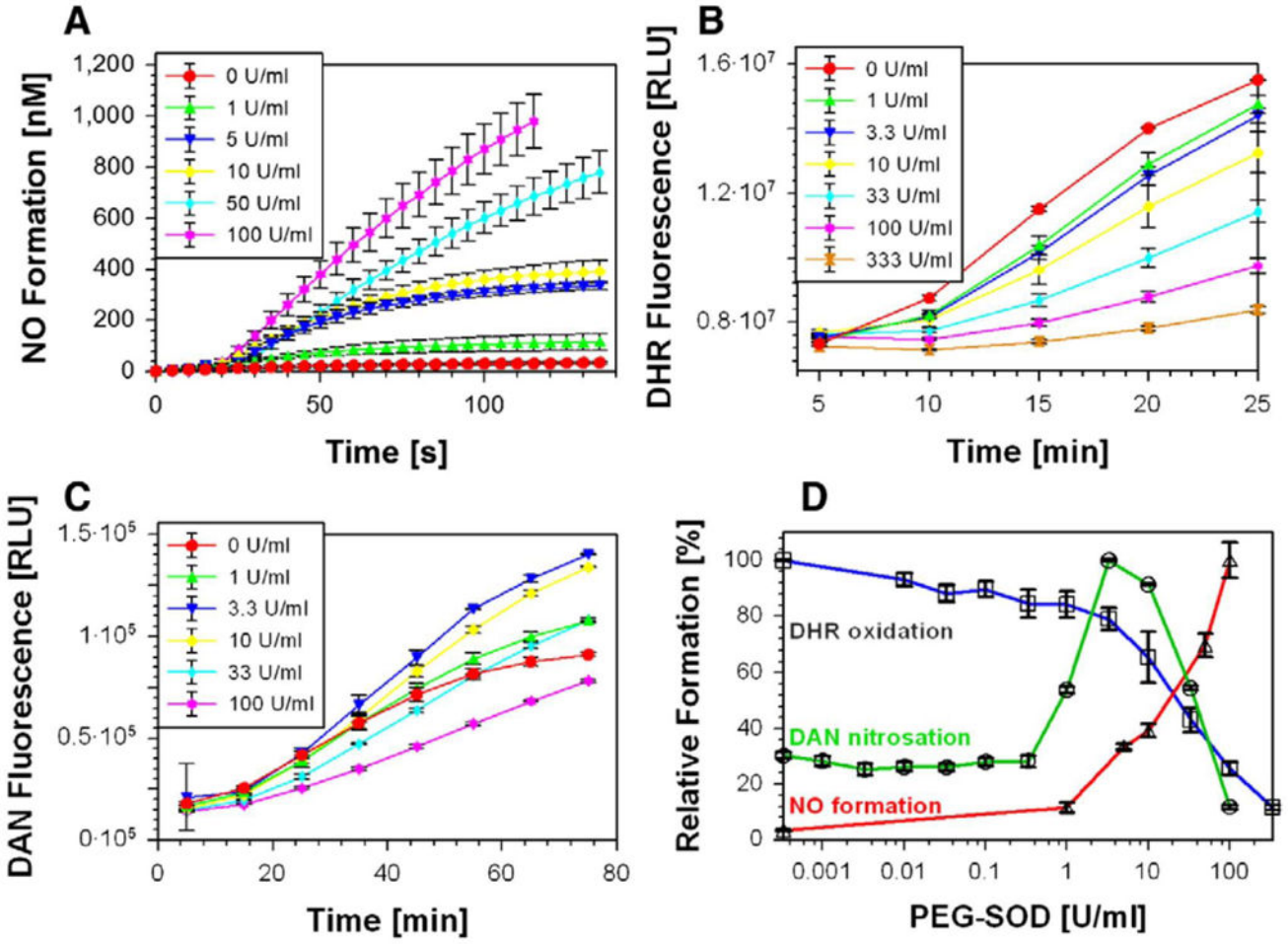

Fig. 4. *N*-nitrosation in the Sin-1/PEG-SOD system

Effects of increasing PEG-SOD concentrations on Sin-1 (100 μM) mediated (**A**) •NO formation, (**B**) peroxynitrite release and (**C**) *N*-nitrosation were measured as described by an •NO electrode, DHR (100 μM) oxidation and DAN (100 μM) fluorescence, respectively. (**D**) All three measured parameters, DHR oxidation, NO formation, and DAN nitrosation were obtained under identical conditions and put into direct correlation. All experiments were performed in 0.1 M potassium phosphate buffer, pH 7.4, at 37°C; values were collected after 90 min incubation; and data are the means±SEM of two or three independent experiments.

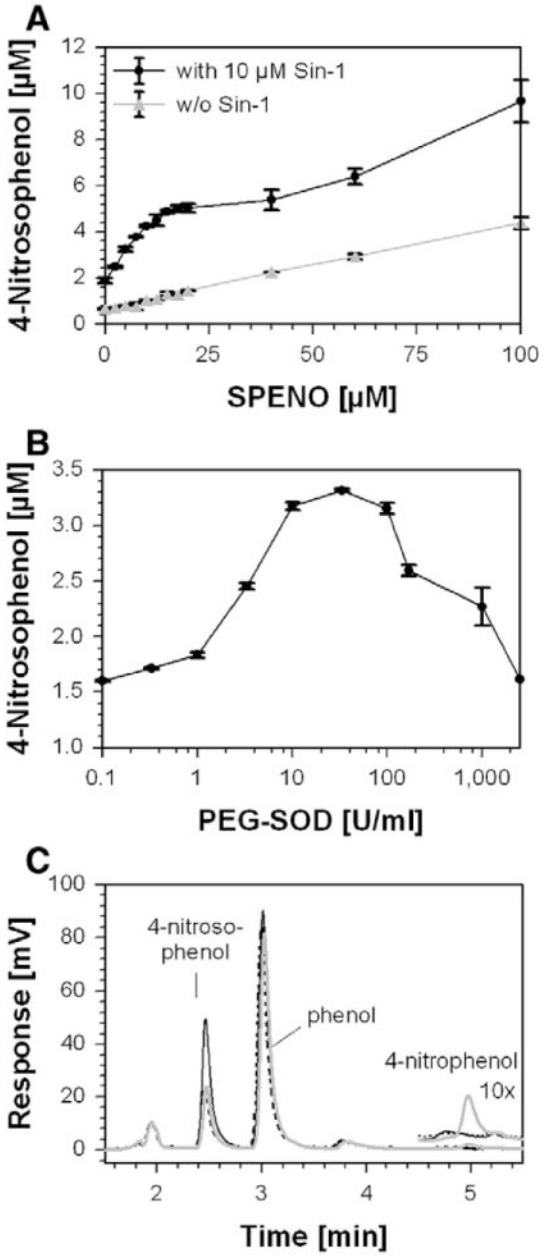

Fig. 5. Determination of *C*-nitrosation in the Sin-1/SPENO and Sin-1/PEG-SOD system

(**A**) Phenol (5 mM) nitrosation was monitored at constant Sin-1 (10 µM) and increasing SPENO concentrations. The effect of SPENO alone was tested in the absence of Sin-1 under similar conditions. (**B**) Phenol (5 mM) nitrosation was monitored at constant Sin-1 (20 µM) and increasing PEG-SOD concentrations. The stable product 4-nitrosophenol was measured by an HPLC-based assay. All experiments were performed in 0.1 M potassium phosphate buffer, pH 7.4, at 37°C; values were collected after 90 min incubation; and data are the means±SEM of two or three independent experiments. (**C**) Representative chromatograms for reaction mixtures of 5 mM phenol, 20 µM Sin-1 and 0.1 (gray line), 33 (black line) or 2500 (dashed line) U/ml PEG-SOD. The inset at 5 min shows a 10-fold magnification of the traces and the formation of 4-nitrophenol.

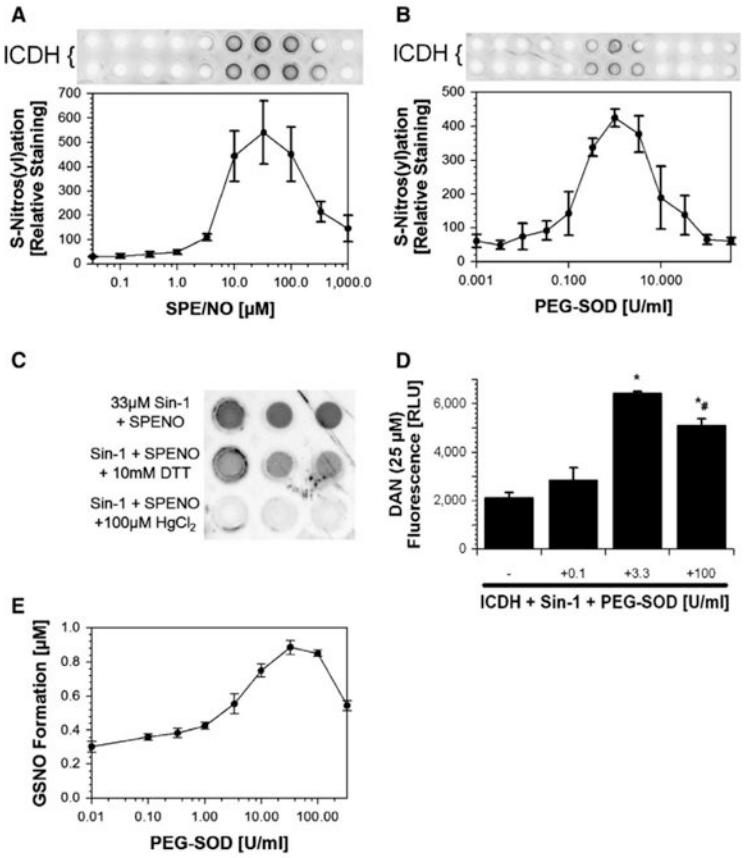

Fig. 6. Determination of *S*-nitros(yl)ation in the Sin-1/SPENO and Sin-1/PEG-SOD system

(**A**) ICDH (5 µM) nitros(yl)ation was monitored at constant Sin-1 (30 µM) and increasing SPENO concentrations. (**B**) ICDH (5 µM) nitros(yl)ation was monitored at constant Sin-1 (30 µM) and increasing PEG-SOD concentrations. (**C**) The specificity of the used *S*-nitrosocysteine-antibody was tested by incubation of a nitrosated sample with either 10 mM DTT or 100 µM $HgCl_2$. The amount of *S*-nitrosocysteine residues was detected by dot-blot technique and three representative dots are shown for each experimental condition. (**D**) Measurement of ICDH (2.5 µM) nitros(yl)ation by $CuSO_4/HgCl_2$-triggered decomposition of *S*-nitrosocysteine and subsequent DAN fluorescence. (E) Determination of S-nitrosoglutathione formation in the Sin-1/PEG-SOD system. GSH (1 mM) nitros(yl)ation was monitored at constant Sin-1 (20 µM) and increasing PEG-SOD concentrations by HPLC-based analysis. All experiments were performed in 0.1 M potassium phosphate buffer, pH 7.4, at 37°C; values were collected after 90 min incubation; and data are the means±SEM of four (**A** and **B**), three (**C** and **D**), or three or four (**E**) independent experiments.